Journal of Applied Electrochemistry **34**: 79–85, 2004.

Structure and properties of electrodeposited silver–bismuth alloys

I. KRASTEV[1,*], T. VALKOVA[1] and A. ZIELONKA[2]
[1]*Institute of Physical Chemistry, Bulgarian Academy of Sciences, 1113 Sofia, Bulgaria*
[2]*Forschungsinstitut für Edelmetalle und Metallchemie, 73525 Schwäbisch Gmünd, Germany*
*(*author for correspondence, e-mail: krastev@ipchp.ipc.bas.bg)*

Received 3 March 2003; accepted in revised form 24 June 2003

Key words: coating properties, electrodeposition, silver–bismuth alloys, structure

Abstract

The elemental and phase compositions, the deposition rate, the structure, and some physico-mechanical properties, such as hardness, wear resistance, roughness and internal stress of electrodeposited coatings of silver–bismuth alloy have been studied. The possibility of deposition of alloy coatings of desired composition depending on the electrolysis conditions and on the composition of the electrolyte used has been demonstrated.With increase in the Bi content in the coatings, hardness and wear resistance decrease, and at Bi contents higher than 50 wt.% the wear resistance remains unchanged. The roughness of the coatings is independent of their Bi content. The alloy coatings reveal a negative (compressive) internal stress. They consist of two phases and are heterogeneous both in the bulk and in the surface layer. A clearly expressed columnar structure is observed, the columns being of different phase composition. This structure is sometimes accompanied by a lamellar structure.The simultaneous deposition of phases with different Bi content leads to self-organization phenomena and formation of wave, spiral and target structures on the electrode surface.

1. Introduction

Bismuth has a number of outstanding properties, which promote interest in its industrial application. One of these properties is the change in electrical resistance when subjected to a magnetic field. Bismuth has a rhombohedral hexagonal crystal lattice and its electrical resistivity depends also on crystal orientation. The metal expands during solidification by about 3.4% compared to the liquid phase, which could be used in the production and densification of composite structures. Although bismuth has a brittle structure at room temperature, at slightly elevated temperature it is quite plastic and ductile. Bismuth and bismuth alloys are used in the production of bearings where the complete insolubility of iron and bismuth prevents any cold welding of the bearing to the shaft [1].

Silver–bismuth alloy is deposited mainly from alkaline electrolytes [2]. The alloy coatings have self-lubrication properties and better solderability [3] due to the lowering of the melting point of silver, as well as increased hardness [4]. The deposition of the alloy from a cyanide electrolyte containing potassium tartrate and KOH has been studied [4]. The composition of the coatings can be changed depending on the cyanide ion content in the electrolyte. At a low KCN concentration, the silver deposition potential is much more positive than that of bismuth. At a high concentration, the deposition potential of Ag is strongly shifted in the negative direction and bismuth becomes the more readily depositing metal and at lower current densities, bismuth deposition is prevailing [4, 5]. Through the proper choice of deposition conditions from such an electrolyte, Ag–Sb alloy coatings of desired composition can be obtained [5].

The alloy coatings with Bi content of up to about 3 wt.% are microscopically homogeneous [4]. They often reveal a lamellar structure with parallel dendritic growth in the direction of the current lines. The other alloys are microscopically diphase structures. In the Bi-rich phases, the bismuth lattice has a practically unchanged lattice constant. X-ray data have shown that the lattice parameter increases up to a bismuth content of about 2.5 wt.%. By measuring the electrical resistance, the maximum solubility of bismuth in silver has been established in alloys containing up to about 2.3 wt.% Bi [4].

The Ag-rich mixed crystals of electrodeposited Ag–Bi alloy could have a higher Bi-content than deduced from the phase diagram at room temperature [4, 6]. The phase diagram of the Ag–Bi system does not reveal the presence of intermediate phases under normal pressure. However, under appropriate conditions, an intermediate phase of the composition Ag_3Bi is metallurgically obtained, the latter being similar to the respective phase in the system Ag–Sb at room temperature [7].

Studies are reported on the catalytic properties of thin bismuth films deposited in vacuum on a glass substrate. Upon deposition of a chemical silver coating on the bismuth film, the change in the optical density of the coating has been measured. A complex phase Ag–Bi has been established, which can be considered as a rhombohedrally textured bismuth film with built in silver atoms. This phase has the characteristics of a superlattice, with a parameter twice as high as that of the normal bismuth lattice, and is catalytically active. The assumption has been made that silver deposition on bismuth takes place in two stages – fast formation of the complex phase Ag–Bi and slow deposition of silver on top as a solid phase without chemical transformations [8].

The present study is aimed at the investigation of the structure and some properties of electrodeposited Ag–Bi alloys and their dependence on electrolysis conditions and alloy composition.

2. Experimental

The electrolyte composition is given in Table 1.

Some coatings were deposited in a glass cell of 100 cm^3 while others, intended for study of the internal stress, were deposited in a cell of 400 cm^3.

Distilled water and *pro analisi* grade reagents were used. Silver anodes were used and coatings were deposited on 0.3 mm thick copper substrates of dimensions 2×1 cm or 7×1 cm. Prior to deposition, the substrates were electrochemically degreased and pickled according to a standard procedure. In some cases, the substrates were silver plated for several minutes in order to prevent contact deposition of silver when dipping into the electrolyte.

The rate of deposition of the alloy and the thickness of the deposited coatings were determined gravimetrically. The alloy composition was determined by X-ray fluorescence analysis (Fischerscope X-RAY HDVM-W). The phase composition of the coatings was determined by X-ray diffraction and the element distribution on the surface and in the bulk was studied by EDXA.

The internal stress, IS, was monitored with the apparatus constructed by Stalzer [9] and the method was described in a previous paper [10]. The method permits *in situ* IS-monitoring during electrodeposition.

The density of the coating was assumed to be the same as that of pure silver.

Table 1. Electrolyte composition

Components	Concentration /g dm^{-3}	Concentration /mol dm^{-3}
Ag as $KAg(CN)_2$	8–32	0.075–0.3
Bi as $BiNO_4$	6–18	0.03–0.09
NaOH	26	0.64
$KNaC_4H_4O_6 \cdot 4H_2O$	60	0.21
KCN	0–120	0–1.85

The microhardness, H_v, of the deposited coatings was measured with a Leitz apparatus Durimet II using a load of 0.245 N at three different positions along the electrode height and the mean arithmetical value of these measurements was calculated. The average value of the roughness, R_a, of the deposited layers was determined by a Perthen profilometer Perthometer.

The wear resistance, A, of the same layers was determined by the Bosch–Weinmann method using the samples from the measurements of the internal stress. The method is described in a previous paper [10]. The wear resistance, A, was determined by the weight loss after 200 cycles using an abrasive band of grade 1000. It is defined as the number of cycles required for the removal of 1 mm^3 of the tested material.

3. Results

3.1. *Coating composition*

Depending on electrolyte composition and C_{KCN}, the deposition potential of silver could be shifted in the negative direction to such an extent that Bi deposition becomes predominant at low current densities [5]. This means that, depending on the concentration of the complex forming agent for silver in the electrolyte, deposition of alloy coatings with Bi-content over a broad range is possible.

Figure 1 shows the effect of both the silver concentration, C_{Ag}, and the KCN concentration, C_{KSCN}, in an electrolyte containing a constant amount of bismuth. In the absence of KCN, pure silver coatings are deposited at low current densities. With increase in current density, the Bi-content in the coating increases up to about 50 wt.% in an electrolyte containing 8 g dm^{-3} Ag and 18 g dm^{-3} Bi.

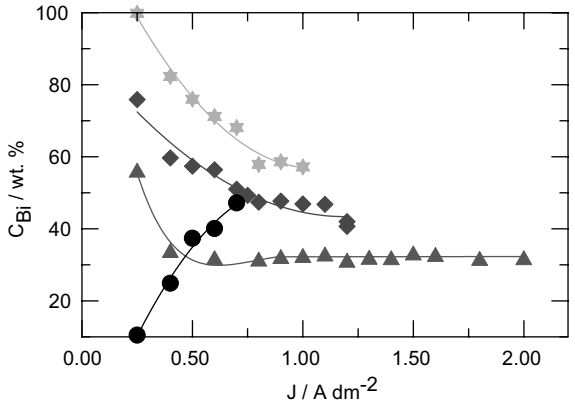

Fig. 1. Influence of current density on alloy bismuth content. C_{Bi} = 18 g dm^{-3}: (●) C_{Ag} = 8 g dm^{-3}; C_{KCN} = 0 g dm^{-3}; (★) C_{Ag} = 8 g dm^{-3}; C_{KCN} = 60 g dm^{-3}; (◆) C_{Ag} = 16 g dm^{-3}; C_{KCN} = 60 g dm^{-3}; (▲) C_{Ag} = 32 g dm^{-3}; C_{KCN} = 60 g dm^{-3}.

The situation drastically changes in the presence of 60 g dm^{-3} KCN–pure bismuth deposits at low current densities. The Ag-content in the alloy increases with the increase in current density, reaching about 60 wt.% at 10 mA cm^{-2}. As expected, higher C_{Ag} result in an increase in alloy silver content. At $C_{Ag} = 32$ g dm^{-3}, the deposition of coatings with almost constant composition is possible over a broad range of current densities.

3.2. *Deposition rate*

Figure 2 shows the effect of the cathodic current density on the alloy deposition rate based on the mass of the coatings deposited. The deposition rate increases linearly with increase in current density regardless of the presence of KCN in the electrolyte. In the presence of KCN, when Bi deposition is prevailing at low currents, the deposition rate is lower. On the one hand, this could be due to the different current yields of the two metals and, on the other hand, to the fact that the thickness of the coating is calculated by the assumption that the latter consists of pure silver. However, taking into account the close density values of the two metals, one can assume that the difference in the two curves is likely due to the difference in the current yields of Ag and Bi. The rates of deposition from the two electrolytes (with and without KCN) become the same in the current density range from 8 to 10 mA cm^{-2} and coatings containing 50–60 wt.% Bi are obtained.

3.3. *Phase composition of the coatings*

The possibility of deposition of coatings with high Bi-content raises the question of their phase composition. According to the phase diagram of the alloy [6], about 3% Bi could be built in the silver crystal lattice and a solid solution is formed. In an electrodeposited Ag–Bi alloy, Raub et al. [4] have established maximal bismuth solubility in silver of about 2.5 wt.%. Despite that the electrodeposited, Ag-rich mixed crystals of the Ag–Bi alloy have a higher threshold bismuth content than that according to the phase diagram at room temperature, it is clear that the high Bi-contents in the coatings studied should be involved in other phases, which can be established by X-ray measurements.

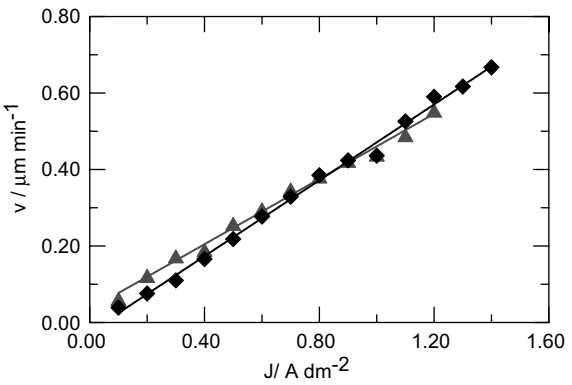

Fig. 2. Influence of current density on alloy deposition rate: $C_{Ag} = 8$ g dm^{-3}; $C_{Bi} = 18$ g dm^{-3}; (▲) $C_{KCN} = 0$ g dm^{-3}; (◆) $C_{KCN} = 60$ g dm^{-3}.

Figure 3 shows X-ray diffractograms of coatings deposited at various current densities from an electrolyte free of KCN, i.e., the coatings are rich in silver. Nevertheless, the coatings appear heterogeneous and the diffractograms reveal the presence of two separate phases. The reflections of the first one correspond to pure Ag, respectively to a solid solution of Bi in Ag, while those of the second one correspond to pure Bi. The analyses in bright and dark surface regions show that the content of pure Bi phase is higher in the dark ones. Within the range of current densities applied, the coatings are heterogeneous and dull.

3.4. *Composition in the coating depth*

A cross section of the coating deposited at 6 mA cm^{-2} and containing 40 wt.% Bi is shown in Figure 4. The regions comprising different phases in the bulk of the coating are clearly seen. The coating has a columnar structure and its appearance could imply prolonged growth of each of the two phases on its own, separate substrate. The heterogeneous regions are macrodispersed and well separated.

Figure 4 also illustrates the surface roughness of the coating as well as the fact that the surface is also heterogeneous and consists of regions comprising different alloy phases. X-ray microanalysis in the light and dark regions reveals that the light regions contain pure Bi (Figure 5) while Ag is prevailing in the dark ones (Figure 6). It can be noticed, at a higher magnification, that a lamellar structure is superimposed on the columnar structure (Figure 7). Quite fine, darker and brighter lamellae are seen along the entire cross section, suggesting differences in the alloy composition within a separate column depending on the coating depth.

3.5. *Microhardness of the coatings*

Figure 8 shows the dependence of the microhardness, H_V, of the deposited layers on the cathodic current density, the latter being proportional to the Ag or Bi amount deposited depending on C_{KCN}. In the absence of KCN and at higher current densities, H_V decreases, suggesting that this parameter worsens with the rise of Bi-content in the coating. The same conclusion can be drawn by considering samples deposited from an electrolyte containing KCN, i.e., the increase in Bi-content results in a decrease of the microhardness of the coating.

Higher C_{Ag} in the KCN-free electrolyte result in coatings richer in silver, which leads to an increase in microhardness, the latter remaining constant within a relatively broader current density range. In addition, compact coatings are obtained at higher current densities, too. The H_v values obtained are in agreement with

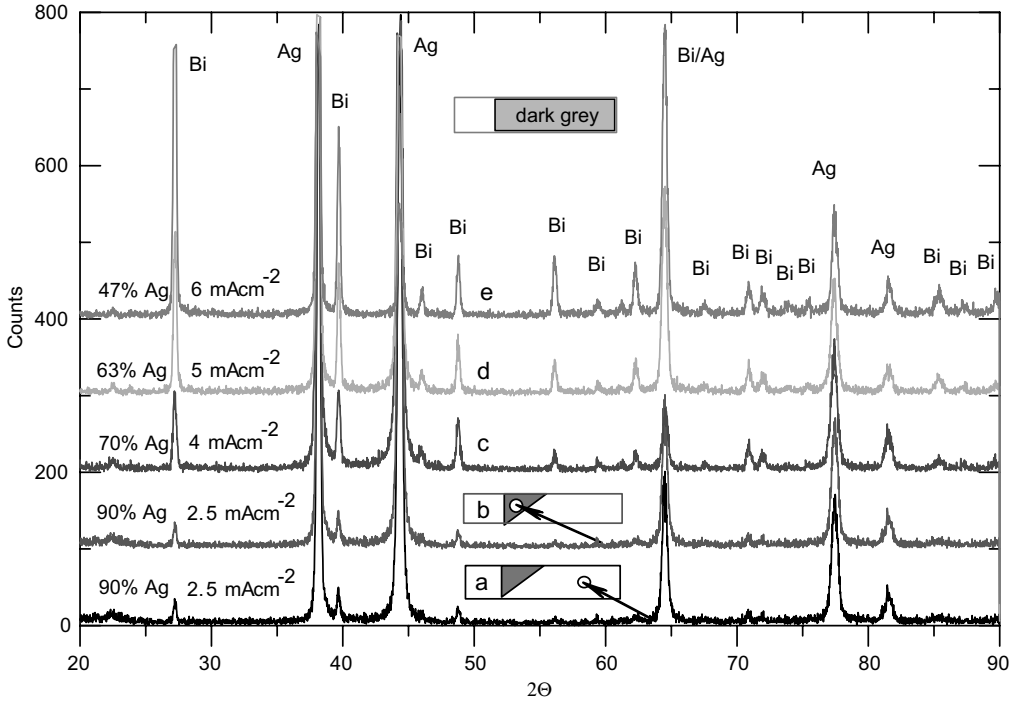

Fig. 3. X-ray diffractograms of alloy coatings deposited at various current densities: (a) $J = 2.5$ mA cm^{-2}; 90 wt.% Ag (light region); (b) $J = 2.5$ mA cm^{-2}; 90 wt.% Ag (dark region); (c) $J = 4$ mA cm^{-2}; 70 wt.% Ag; (d) $J = 5$ mA cm^{-2}; 63 wt.% Ag; (e) $J = 6$ mA cm^{-2}; 47 wt.% Ag.

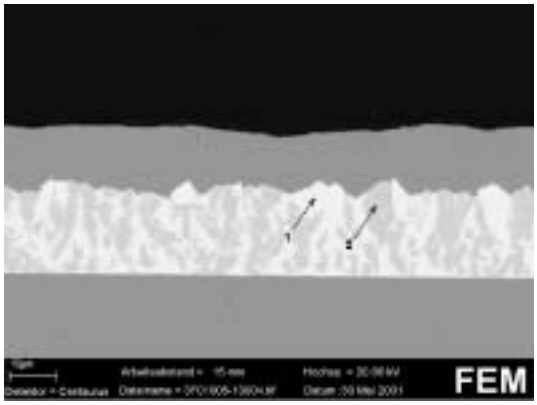

Fig. 4. Cross section of an alloy coating: $C_{Ag} = 16$ g dm^{-3}; $C_{Bi} = 18$ g dm^{-3}; $C_{KCN} = 60$ g dm^{-3}; $J = 6$ mA cm^{-2}; 53.7 wt.% Bi.

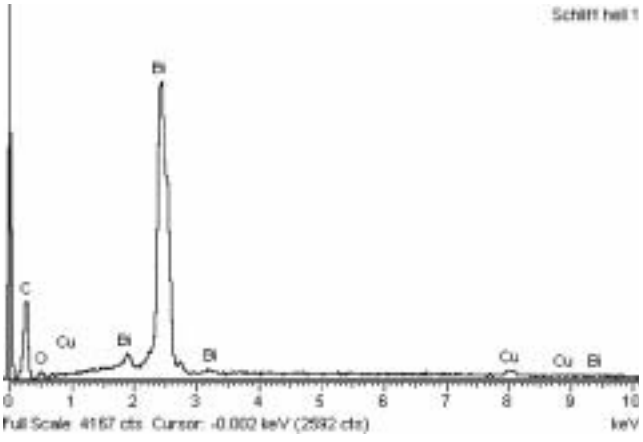

Fig. 5. EDXA-spectrum at Point 1 in Figure 4.

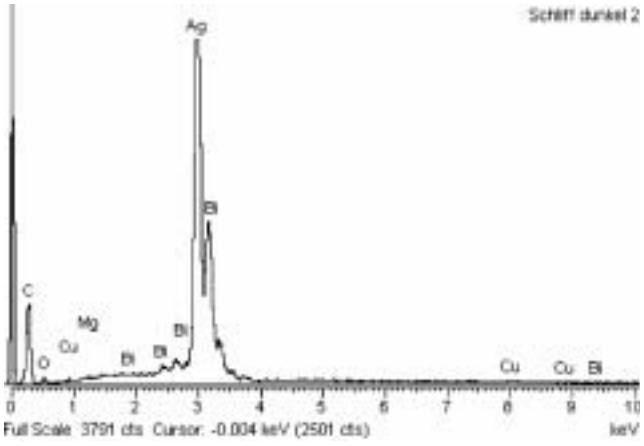

Fig. 6. EDXA-spectrum at Point 2 in Figure 4.

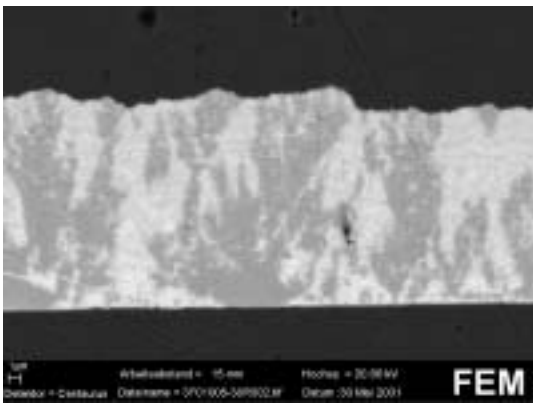

Fig. 7. Cross-section of an alloy coating: $C_{Ag} = 32$ g dm^{-3}; $C_{Bi} = 18$ g dm^{-3}; $C_{KCN} = 65$ g dm^{-3}; $J = 6$ mA cm^{-2}; 29 wt.% Bi.

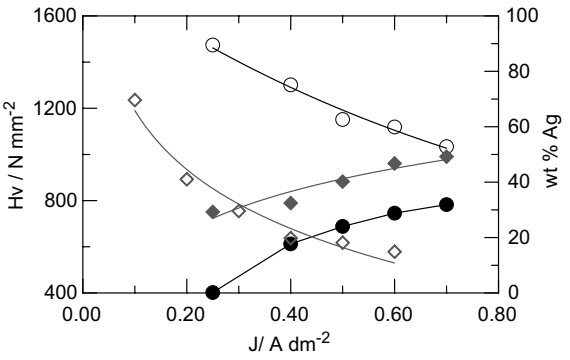

Fig. 8. Influence of current density on microhardness and composition of the deposited layers: C_{Ag} = 8 g dm^{-3}; C_{Bi} = 18 g dm^{-3}; C_{KCN} = 60 g dm^{-3}: (●) *Ag* content; (◆) H_v; C_{KCN} = 0 g dm^{-3}: (○) *Ag* content; (□) H_v.

the data reported by other authors [4] who state that the Ag-rich Ag–Bi alloys have a microhardness within the limits 90–180 kg mm^{-2} (880–1760 N mm^{-2}), which is considerably higher than that of cast alloys of the same composition.

3.6. *Roughness of the coatings*

The roughness, $R_{a,}$ of the deposited coatings is almost constant within the entire range of current densities studied and is of the order of 2 μm. The rise in C_{Ag} at constant C_{Bi} does not lead to substantial changes in R_a. The coatings are dull within the entire range of current densities applied. The Bi-rich coatings deposited in the presence of KCN in the electrolyte are slightly rougher.

3.7. *Wear resistance of the coatings*

The wear resistance, A, of the alloy coatings as dependent of their Bi-content is depicted in Figure 9. At quite low Bi-contents in the alloy, a slight increase of the wear resistance is possible in the concentration range where the two metals form a solid solution. The increase in Bi-content results in the obtaining of heterogeneous coatings with decreased wear resistance, the latter reaching a constant value at about 50 wt.% Bi in the coating and remaining almost unchanged in Bi-richer coatings (up to 100 wt.%), which can be obtained at a sufficiently high C_{KCN}. This constant value of A in the range of 50–100 wt.% Bi probably corresponds to the wear resistance of pure bismuth.

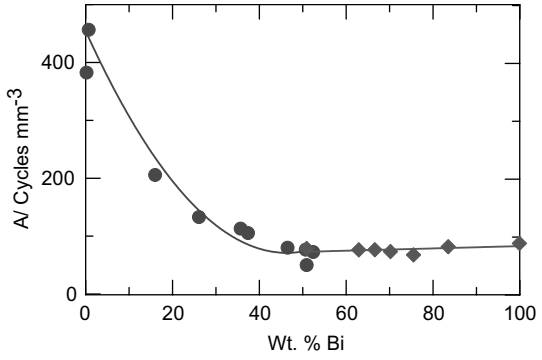

Fig. 9. Dependence of alloy wear resistance on Bi-content in the alloy: C_{Ag} = 8 g dm^{-3}; C_{Bi} = 18 g dm^{-3}; (●) C_{KCN} = 0 g dm^{-3}; (◆) C_{KCN} = 60 g dm^{-3}.

3.8. *Internal stress of the coatings*

Figures 10 and 11 show the changes in the sensor signal caused by the change of the internal stress IS, of the coating with time. The internal stress itself is proportional to the slope of the curve obtained and can be calculated by means of the respective equation [9] accounting for the substrate size, the material type, and the coating thickness. The stress appearing in pure

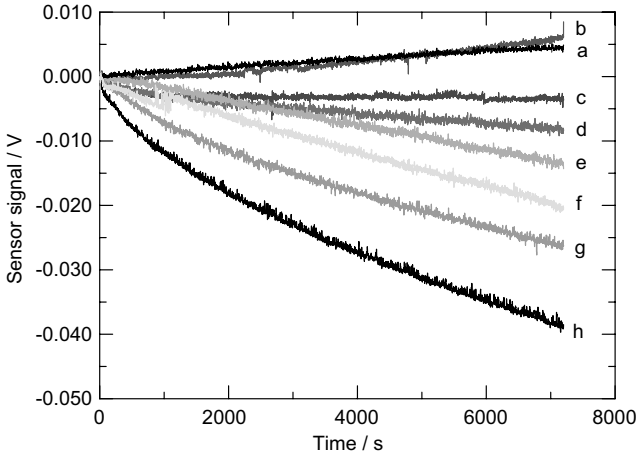

Fig. 10. Change in the sensor signal with time at low current densities: C_{Ag} = 8 g dm^{-3}; C_{Bi} = 18 g dm^{-3}; (a) 1 mA cm^{-2}; 0.5 wt.% Bi; (b) 2 mA cm^{-2}, 0.7 wt.% Bi; (c) 3 mA cm^{-2}; 18.9 wt.% Bi; (d) 4 mA cm^{-2}, 25.9 wt.% Bi; (e) 5 mA cm^{-2}; 34.9 wt.% Bi; (f) 6 mA cm^{-2}, 40.4 wt.% Bi; (g) 7 mA cm^{-2}; 45.0 wt.% Bi; (h) 8 mA cm^{-2}, 50.0 wt.% Bi.

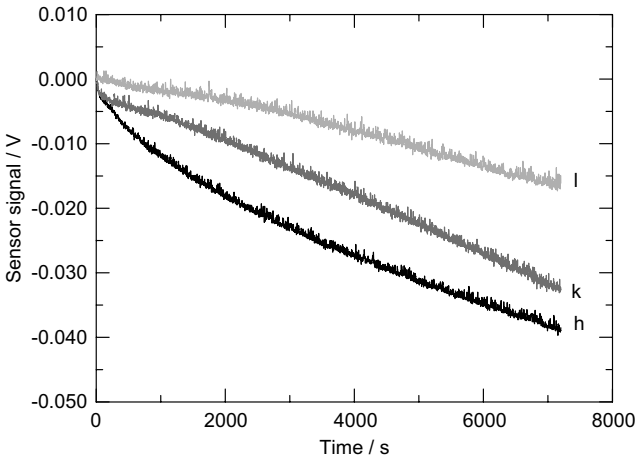

Fig. 11. Change in the sensor signal with time at high current densities: C_{Ag} = 8 g dm^{-3}; C_{Bi} = 18 g dm^{-3}; (h) 8 mA cm^{-2}, 50.0 wt.% Bi; (k) 11 mA cm^{-2}, 51.0 wt.% Bi; (l) 12 mA cm^{-2}, 54.0 wt.% Bi.

Ag deposits (1–2 mA cm^{-2}) is positive [10]. Bismuth codeposited at low current densities is built in the Ag crystal lattice and has a stretching effect on the latter, resulting in the recording of a negative internal stress, i.e., compressive stress. It should be noted that Bi is built in the Ag lattice within a relatively narrow range of concentrations of this element in the coating, so that the increase in IS with the further increase in current density should be related to the appearance of a negative IS in the separate Bi-phase included in the heterogeneous coating. The increase in IS is observed at current densities up to 8–9 mA cm^{-2}; under these conditions, coatings containing up to 50 wt.% Bi are obtained (compare with Figure 1). The further increase of the current density leads to a drop of IS which cannot be related to the appearance of a new phase since, under these conditions, the heterogeneous coating contains just a solid Ag–Bi solution and a pure Bi-phase. The decrease of IS is most likely related to the appearance of rougher, spongy or dendrite-like coatings at higher current densities.

3.9. *Surface of the coatings*

The surface of the coatings is dull, grey, and becomes dark grey to black with increase in the Bi-content. When the coating is deposited in the absence of KCN and its Bi-content is high, its surface is heterogeneous in colour and consists of dark and light regions, which could sometimes be ordered; such a coating is shown in Figure 12. Straight waves, spirals and target structures are observed on the electrode surface. The Bi-content in such coatings varies between 50 and 60 wt.%. The samples reveal heterogeneity also in the coating depth (compare with Figures 4 and 7). During deposition, moving structures are not visually observed, i.e., the propagation rate of the fronts is low, and substantially lower than that in the Ag–Sb system [11–18]. Judging from the large regions (Figure 13) occupied by the two phases (compare with Figures 4 and 7), one can conclude that the propagation rate of the fronts is so low because the effect of the substrate on the surface structure is possibly much stronger than that of the natural convection in the electrolyte during electrolysis.

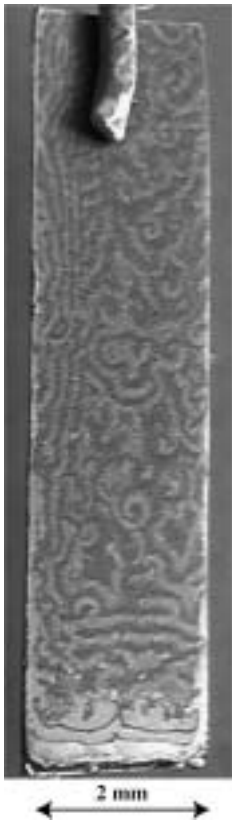

Fig. 12. Surface of an alloy coating; electrode dimensions 10 × 2 mm: $C_{Ag} = 8$ g dm^{-3}; $C_{Bi} = 18$ g dm^{-3}; $J = 9$ mA cm^{-2}.

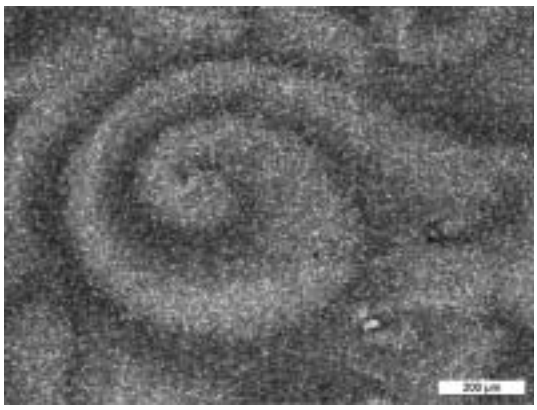

Fig. 13. Surface of an alloy coating: $C_{Ag} = 8$ g dm^{-3}; $C_{Bi} = 18$ g dm^{-3}; $J = 4$ mA cm^{-2}; 40 wt.% Bi.

4. Conclusions

- The possibility of obtaining coatings of desired composition depending on the electrolyte composition and on the electrolysis conditions is shown.
- The increase in Bi-content in the alloy leads to a decrease in the hardness and wear resistance of the coatings and does not substantially affect their roughness.
- Tensile stress is observed in pure Ag deposits. The Bi containing coatings are characterized by negative IS (compressive stress).
- The heterogeneity in the bulk of the coatings is clearly shown by their columnar structure, the columns being characterized by different elemental and phase compositions. A lamellar structure is sometimes superimposed on the columnar one.
- At high Bi-contents, the heterogeneity in the surface layer of the coatings leads to the formation of spatio-temporal structures in the shape of straight waves, spirals and target patterns, resembling the structures observed in Ag–In and Ag–Sb alloys.

Acknowledgements

The present studies are part of a joint research project between the Institute of Physical Chemistry of the Bulgarian Academy of Sciences, Sofia and Forschungsinstitut für Edelmetalle und Metallchemie, Schwäbisch Gmünd. The authors express their gratitude to Deutsche Forschungsgemeinschaft for financial support of project 436 BUL 113/97/0-2.

References

1. GB Patent 590 412 (1947).
2. P.M. Vjacheslavov, 'Nowie elektrokhimicheskie pokritija' (Lenizdat, Leningrad, 1972), p. 264 (in Russian).
3. S.N. Vinogradov and A.N. Berzhinskaja, Sowjetunion conference 'Elektrokhimicheskoe osazhdenie i primenenie pokritij dragocennimi metallami', Charkov, 24–26 Okt. 1972, Abstracts, p. 43 (in Russian).
4. E. Raub and A. Engel, *Zeitschrift für Metallkunde* **41** (1950) 485.
5. I. Krastev, T. Valkova and A. Zielonka, submitted in JAE, (2003).
6. M. Hansen and K. Anderko, 'Strukturi dwojnih splawow' (Metallurgizdat, Moscow, 1962), p. 23 (in Russian).
7. V. Degtyareva, G. Nover, D. Schoenbohm and H. Klaper, *Solid State Commun.* **106**(5) (1998) 259.
8. V.S. Gurin, The 1997 Joint International Meeting of the Electrochemical Society and The International Society of Electrochemistry, Paris, Abstracts, 552.
9. M. Stalzer, *Metalloberfläche* **18** (1964) 263.
10. I. Krastev, N. Petkova and A. Zielonka, *J. Appl. Electrochem.* **32**(7) (2002) 811.
11. I. Kristev and M. Nikolova, *J. Appl. Electrochem.* **16** (1986) 875.
12. I. Krastev, M.E. Baumgärtner and Ch.J. Raub, *Metalloberfläche* **46**(2) (1992) 63.
13. I. Krastev, M.E. Baumgärtner and Ch.J. Raub, *Metalloberfläche* **46**(3) (1992) 115.
14. I. Krastev and M.T.M. Koper, *Physica A* **213** (1995) 199.
15. H.R. Khan, O. Loebich, I. Krastev and Ch.J. Raub, *Trans. Inst. Metal Finish.* (*UK*) **72**(4) (1994) 134.
16. I. Krastev, *Bulg. Chem. Commun.* **29**(3/4) (1997) 586.
17. S. Nakabayashi, I. Krastev, R. Aogaki and K. Inokuma, *Chem. Phys. Lett.* **294** (1998) 204.
18. S. Nakabayashi, K. Inokuma, A. Nakao and I. Krastev, *Chem. Lett.* (2000) 88.